Numerical Weather Prediction

Soil state and surface hydrology diagnosis based on MOSES in the Met Office Nimrod nowcasting system

Forecasting Research Technical Report No. 428

R.N.B. Smith, E.M. Blyth, J.W. Finch, S. Goodchild, R.L. Hall and S. Madry

email: nwp_publications@metoffice.com

©Crown Copyright

Soil state and surface hydrology diagnosis based on MOSES in the Met Office Nimrod nowcasting system

R.N.B. Smith[(1)], E.M. Blyth[(2)], J.W. Finch[(2)],
S. Goodchild[(3)], R.L. Hall[(2)] and S. Madry[(1)]

(1) Met Office, Joint Centre for Hydro-Meteorological Research, Wallingford, OX10 8BB, United Kingdom
(2) Centre for Ecology and Hydrology, Joint Centre for Hydro-Meteorological Research, Wallingford, OX10 8BB, United Kingdom
(3) Met Office, FitzRoy Road, Exeter, EX1 3PB, United Kingdom

Abstract

A system has been developed and made operational at the Met Office for the real-time diagnosis of soil state and surface hydrology. It is based on the Met Office Surface Exchanges Scheme (MOSES) modified to take account of unresolved soil and topographic heterogeneity when calculating surface runoff by incorporating a Probability Distributed Moisture (PDM) scheme developed by the Centre for Ecology and Hydrology. The implementation of MOSES-PDM in the Met Office's Nimrod nowcasting system is described. High resolution soil characteristics and land cover data together with Nimrod's analyses of precipitation amount and type, cloud cover and near-surface atmospheric variables are used to drive MOSES-PDM. Hourly values are calculated of snowmelt, runoff, net surface radiation, evaporation, potential evaporation, soil temperature, soil moisture and soil moisture deficit on a 5km grid.

1. Introduction

Estimation of the amount and state of moisture in the rooting zone of soils (the top few metres) is required for a variety of purposes. Soil moisture is a major factor in the partitioning of available energy into sensible and latent heat fluxes into the atmosphere and so Numerical Weather Prediction (NWP) models need an accurate soil moisture field as one of their lower boundary conditions. NWP models are prone to errors in their simulations of precipitation and cloud cover which can lead to drift in the model's own soil moisture which in turn feeds back to induce further errors in atmospheric variables. Estimates of soil moisture based on observations of precipitation and/or other meteorological variables, and produced independently of the NWP model, can therefore be beneficial if used to update and correct the NWP model's soil moisture (Rhodin *et al.*, 1999).

Soil moisture is the most important antecedent condition which influences how much rainfall runs off into rivers and potentially causes floods. An operational system is therefore desirable which partitions observed precipitation between surface runoff and soil infiltration and also calculates the amounts of soil moisture which return to the atmosphere through transpiration and evaporation and which drain away out of the root zone to form ground water. Such a system would also be a natural candidate for directly coupling to river flow and flood forecasting models.

Water resource managers also need to know the amounts of water entering and leaving the soil. Those working in agriculture benefit from knowing about soil moisture so that they can decide if and when to plant and irrigate crops. The strength of the soil depends partly on its moisture content. Consequently the insurance industry are showing increasing interest in reliable estimates of soil moisture to assess claims for building subsidence. The military need to make decisions about the ability of terrain in the regions of their operations to support the manoeuvres of heavy vehicles such as tanks (the so-called "trafficability" of the terrain which depends on soil strength).

To provide up-to-date soil moisture fields for all these purposes on national, regional or global scales directly from observations is not possible. In situ probes are sparsely distributed and their moisture measurements have limited spatial validity because of natural soil heterogeneity. Remotely sensed microwave brightness temperatures can give estimates of soil moisture to a limited depth (Burke and Simmonds, 2001b) but there are problems with retrieval below vegetation, so soil and vegetation models have to be used which brings us into the realm of combining models and observations.

The method of combining observations with models commonly used in meteorology is variational data assimilation. Recent application of this to soil moisture analysis for NWP modelling is described by Rhodin *et al*. (1999), Hess (2001) and Seuffert *et al*. (2003). These authors use differences between model and observed screen level humidity and temperature to deduce adjustments to the model's soil moisture. This technique has validity if the use of the resulting soil moisture field is restricted to providing a lower boundary condition to the NWP model. This is because the soil moisture is essentially being regarded as a continuously 'tuned' parameter field to minimise errors in simulations of atmospheric variables. The technique may be questioned for applications where the soil moisture and surface hydrology themselves are the primary focus. The soil moisture may be adjusted with data assimilation techniques to correct for errors in the atmospheric model, for example cloud errors. For this reason a method of soil moisture diagnosis by direct driving of a

physical model may be preferable when the soil moisture and runoff are used for the applications outlined above. Most of the users of soil moisture and runoff estimates also require higher resolution than current NWP models.

An operational service has been provided by various versions of the Met Office Rainfall and Evaporation Calculation System (MORECS) since 1978 (Hough and Jones, 1997). MORECS uses rain gauge observations and synoptic weather station observations of temperature, humidity, wind and sunshine to update a surface and subsurface water balance model. Although pioneering in its day, MORECS has reached its limit of adequacy to provide high resolution real-time soil moisture and runoff information. It provides daily updates on a 40km resolution grid, does not use remotely sensed data, is not designed to disseminate its products using modern electronic transmission methods and is based on modelling techniques which have not kept pace with those used in the land surface components of NWP and climate models. There are also difficulties in transforming the soil moisture deficit from MORECS into a soil moisture profile for updating NWP models.

Rather than invest effort in a large upgrade to MORECS it was decided to bring together two major developments of the middle and late 1990s, namely the Met Office's Nimrod nowcasting system (Golding, 1998) and the Met Office Surface Exchanges Scheme (MOSES) (Cox *et al*., 1999 and Essery *et al*., 2003). Nimrod was designed to provide analyses and short-range forecasts of precipitation and other meteorological variables based on optimal combinations of remotely sensed, modelled and in situ data. MOSES was designed to calculate the fluxes of water and energy (and also carbon in some climate simulation applications) at the land surface and in the root zone of the soil.

The remainder of this paper describes how MOSES has been enhanced by including a new surface runoff production component based on the Probability Distributed Moisture (PDM) scheme developed at the Centre for Ecology and Hydrology (Section 2) and by the calculation of some additional user-focussed outputs (Section 4). Section 3 describes how MOSES-PDM was integrated into the Nimrod system thereby enabling MOSES-PDM to be driven by Nimrod's high resolution analyses of precipitation, cloud and near-surface atmospheric variables and to provide hourly updates of soil moisture, snowmelt, runoff and evaporation. Note that this implementation of MOSES-PDM in Nimrod involves a direct driving of a physical land surface model by analysed fields and does not attempt to use variational data assimilation techniques as outlined above.

2. The surface and subsurface process model

2.1 MOSES

The Met Office Surface Exchange Scheme (MOSES) is the basis of the facility to diagnose the hydrological state of the surface and soil from Nimrod's analyses of near-surface meteorological variables. MOSES was originally developed for a General Circulation Model (GCM) to calculate the surface-to-atmosphere fluxes of heat and water and to update the surface and subsurface variables which affect these fluxes (Cox *et al*., 1999). MOSES is a major advance on simple "bucket" models (Carson, 1982) and a significant improvement on the intermediate complexity model used previously in the Met Office's GCM and Numerical Weather Prediction (NWP) models (Warrilow and Buckley, 1989). It is worth noting that MORECS (Thompson *et al*., 1981; Hough and Jones, 1997), which has hitherto been the Met Office's operational tool for diagnosing soil moisture deficits from observed data, is

also a variant of the bucket type of model since it only allows runoff when water stores are full.

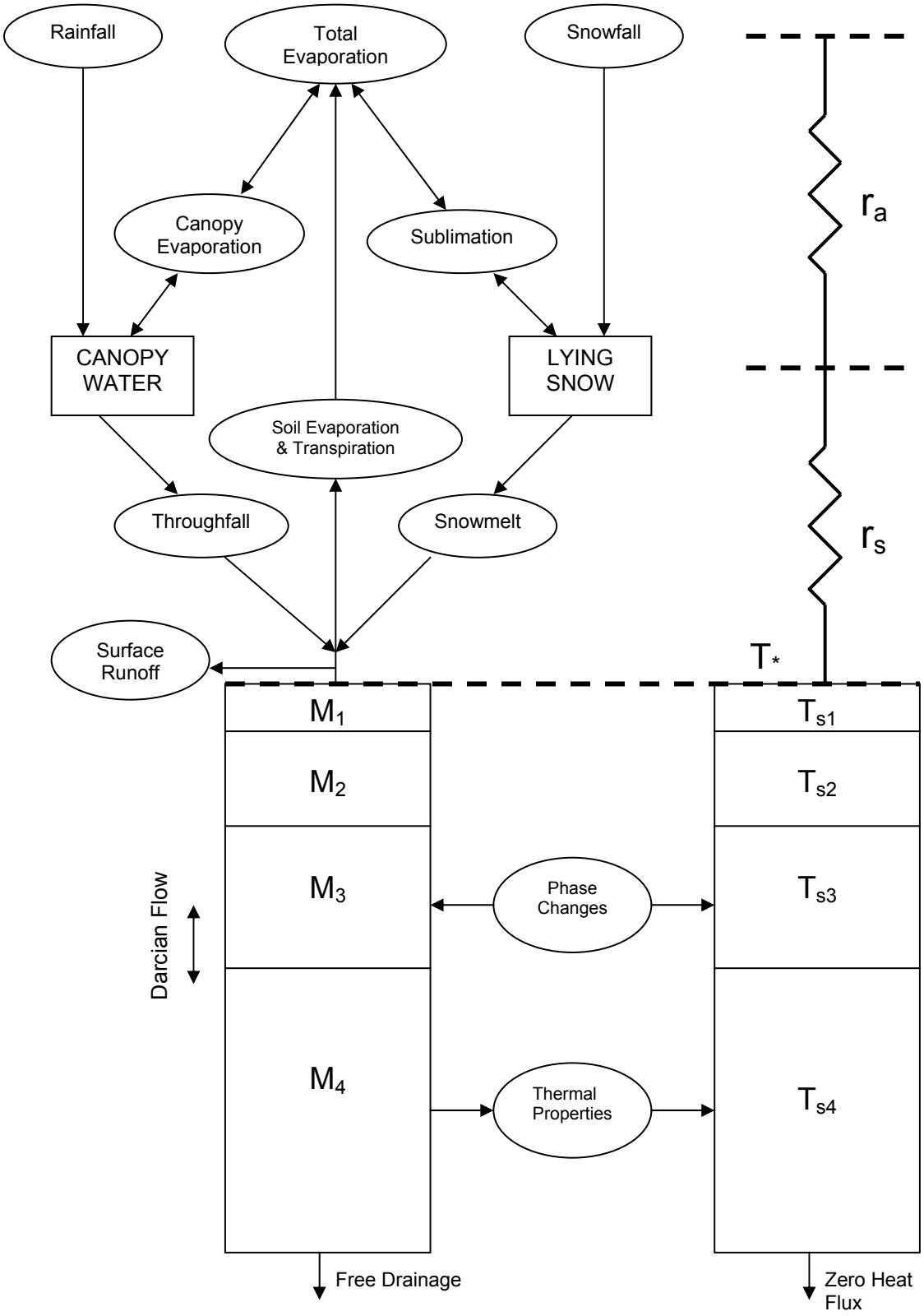

Figure 1. Schematic representation of the Met Office Surface Exchanges Scheme (MOSES), after Figure 1 of Cox *et al*. (1999). Each soil layer has a temperature, T_{Sk}, and moisture content M_k. The surface skin temperature is T_*. r_a is the aerodynamic resistance to evaporation and r_s is the surface resistance.

Figure 1 (after Figure 1 in Cox *et al*. (1999)) shows, in schematic form, the main processes represented and the water and heat stores in MOSES. There are four soil layers each with a temperature, T_S, and moisture content, M. As currently configured, the four soil layers have thicknesses, from the surface downwards, of 0.1, 0.25, 0.65 and 2.0 metres. On the surface there are lying snow and canopy water stores. The canopy water is the rainfall intercepted by plant leaves which is available for free evaporation. The method of partitioning precipitation into canopy interception and throughfall is described by Dolman and Gregory (1992).

The total moisture flux from the surface is made up of evaporation from the canopy water store, E_c, transpiration by vegetation, E_v, bare soil evaporation, E_b and sublimation from the lying snow surface, E_σ. Canopy evaporation and sublimation are subject to aerodynamic resistance, r_a, only, whereas transpiration and bare soil evaporation are subject to both the aerodynamic resistance and a surface resistance, r_s. For vegetated surfaces the surface resistance is set to an interactive canopy or "bulk stomatal" resistance, r_c. The reciprocal of r_c, the conductance, g_c, is calculated by a photosynthesis model (Cox *et al*., 1998) and depends on surface air temperature, humidity deficit, incident radiation and vegetation type. Both the canopy and bare soil surface conductances also include dependencies on the soil moisture content via a soil moisture availability factor, β, (see Section 4.2 below and Cox *et al*. (1999)). The aerodynamic resistance is a function of surface roughness, wind speed and atmospheric surface layer stability.

MOSES assumes an energy balance at the land-atmosphere interface so that the net downward radiation at the surface is equal to the sum of the sensible and latent heat fluxes from the surface into the atmosphere, the conductive heat flux from the surface to the centre of the top soil layer and the latent heat required for any surface snowmelt. When snow is lying, melting occurs when the surface temperature or the snow layer temperature exceed the freezing point of water. Sufficient snowmelt occurs to ensure that the surface energy balance is satisfied with the surface temperature equal to the freezing point.

The soil thermodynamics in MOSES is represented by diffusive heat exchanges between the soil layers and by the heat transported between the layers by the fluxes of moisture. The soil thermal characteristics are functions of soil moisture (liquid and frozen). Soil water phase changes are also represented and the associated latent heat is included in the thermodynamic calculations. Further details of the soil thermodynamics are given by Cox *et al*. (1999).

The soil hydrology component of MOSES is based on a finite difference form of the Richards equation (Richards, 1931). The vertical discretisation for soil hydrology is the same as that for the thermodynamics, i.e. the positions of the moisture levels and layers coincide with those of the temperatures. The prognostic soil moisture content, M ($kg_{(water)}\ m^{-2}$), is the sum of frozen and unfrozen components,

$$M = \rho_w \Delta z \theta_{sat} \left(S_f + S_u \right) \qquad (1)$$

where S_f and S_u are the amounts of frozen and unfrozen water in the layer as a fraction of the amount of liquid water at saturation; θ_{sat} is the liquid soil moisture volumetric concentration at saturation ($m^3_{(water)}\ m^{-3}_{(soil)}$); ρ_w is the density of liquid water ($kg_{(water)}\ m^{-3}_{(water)}$) and Δz is the thickness (m) of the soil layer. The diffusive fluxes of soil moisture between the layers, W ($kg_{(water)}\ m^{-2}\ s^{-1}$), are given by the Darcy equation,

$$W = K\left(\frac{\partial \Psi}{\partial z} + 1\right) \quad (2)$$

where K is the hydraulic conductivity ($kg_{(water)}$ m^{-2} s^{-1}) and Ψ is the soil water suction (m). These quantities are given in terms of their saturation values by the formulae of Clapp and Hornburger (1978),

$$K = K_{sat} S_u^{2b+3} \quad (3)$$

$$\Psi = \Psi_{sat} S_u^{-b} \quad (4)$$

where K_{sat}, Ψ_{sat} and b are empirical soil dependent parameters. (See Section 3.5 for the specification of soil type dependent parameters.) The top boundary condition for the MOSES soil hydrology is,

$$W_0 = P_f + S_m - Y_s \quad (5)$$

where W_0 is the water flux which enters the soil at the surface and P_f, S_m and Y_s are the throughfall, snowmelt and surface runoff respectively ($kg_{(water)}$ m^{-2} s^{-1}). The lower boundary condition assumes free drainage (Cox *et al*., 1999).

Evapotranspiration through plants extracts soil moisture directly from each soil layer via roots and bare soil evaporation depletes moisture from the top soil layer. The ability of roots to access moisture in each soil layer is determined by a root density distribution; root density is assumed to follow an exponential distribution with depth (Thornley and Johnson, 1990, and see Section 4.2 below).

2.2 MOSES-2

MOSES was upgraded to MOSES-2 by Essery *et al*. (2003) to represent sub-grid heterogeneity of the land cover. In MOSES-2 separate upward radiative fluxes, sensible heat fluxes, moisture fluxes, surface temperatures, lying snow amounts and canopy water amounts are calculated for each land surface type represented. These are then aggregated to form a gridsquare mean with weightings equal to the fractions of each type in the gridsquare. Land surface schemes which represent surface heterogeneity in the manner of MOSES-2 are often called "tiled" or "mosaic" schemes. Since information for different surface types is useful to users and because of the greater accuracy of tiled land surface schemes, MOSES-2 was taken as the basis of the soil and surface hydrology component of the Nimrod nowcasting system. The land surface types represented in the Nimrod implementation are six vegetation types (broadleaf trees, needleleaf trees, temperate C_3 grass, tropical C_4 grass, crops and shrubs) and four non-vegetated surface types (urban, inland open water, bare soil and ice). Only one generic crop type has been included so far. With each type of vegetation is associated a canopy height, a snow-free roughness length and a canopy water capacity which are parametrized functions of the Leaf Area Index (LAI). Each vegetated tile also has a root density distribution depending on the plant type. Evaporation from the bare soil tile is drawn from the top soil layer only. Lakes and urban surfaces are represented very simply: lake tiles are smooth and perpetually wet; urban tiles are rough and have a small surface water capacity from which evaporation can occur. There is no water extraction from the soil layers for urban tiles.

2.3 MOSES-PDM

Although MOSES-2 represents the sub-gridscale heterogeneity of land surface cover, it does not represent any heterogeneity of the soil hydrology on scales less than those resolved by the grid-squares. In their standard versions, MOSES and MOSES-2 give a non-zero surface runoff from canopy throughfall and snowmelt only when the sum of the latter two quantities exceeds the infiltration rate of the soil (Dolman and Gregory, 1992); they do not represent saturation excess runoff. In temperate zones, precipitation is rarely heavy enough to exceed infiltration rate and so the surface runoff simulated by MOSES and MOSES-2 is erroneously low. Surface saturation runoff is significantly affected by heterogeneity in soil water holding capacity. The Probability Distributed Moisture (PDM) scheme of Moore (1985) was incorporated into MOSES-2 by Blyth (2002) to represent saturation runoff and unresolved soil heterogeneity, thereby forming what will be henceforth be called "MOSES-PDM". MOSES-PDM is the surface and subsurface process model implemented in the Nimrod nowcasting system.

The PDM scheme assumes that within an area large enough to warrant a representation of heterogeneity, soils have a distribution of water holding capacity, c ($kg_{(water)}\ m^{-2}$), described by the cumulative distribution function F(c) given by,

$$F(c) = 1 - \left(1 - \frac{c}{c_{max}}\right)^{B} \qquad 0 \le c \le c_{max} \qquad (6)$$

B is a parameter describing the degree of spatial variability, a value of 1 is currently used everywhere. Note that F(c) is the fractional area with capacities ≤ c (Moore, 1985). A schematic PDM distribution of soil water stores is shown in Figure 2. (The function given in equation (6) is continuous; the schematic form of the function shown in Figure 2, particularly its discretisation, is solely to help visualise the concept of a distribution of water holding elements.) c_{max} in equation (6) is a maximum soil capacity.

It is assumed that each MOSES gridsquare has a distribution of water holding elements given by the PDM scheme. c_{max} is then related to the gridsquare saturated volumetric soil moisture concentration, θ_{sat} ($m^3_{(water)}\ m^{-3}_{(soil)}$), by equating the maximum amount of soil water per square metre of the gridsquare given by MOSES and the PDM formulation respectively,

$$\rho_w \theta_{sat} \Delta z_{PDM} = \int_0^{c_{max}} c f(c) dc \qquad (7)$$

where f is the probability distribution function associated with F, i.e. f(c)=F′(c). Δz_{PDM} is the depth (m) of soil over which the PDM is assumed to apply. This depth is now set to 1 metre, which differs from the assumption of Blyth (2002) that the PDM applies only over the top soil layer in MOSES, i.e. the top 0.1 m of soil. The mean soil moisture in the top metre of soil is thought to be more appropriate for determining runoff from the PDM. Evaluating the integral in equation (7) gives,

$$c_{max} = (B+1)\rho_w \theta_{sat} \Delta z_{PDM} \qquad (8)$$

The critical storage capacity below which all stores are full (see Figure 2), c_*, is related to the mean soil moisture volumetric concentration, θ_{PDM}, over the depth

Δz_{PDM} by equating the actual amount of soil water per square metre of the gridsquare as given by MOSES and the PDM formulation respectively,

$$\rho_w \theta_{PDM} \Delta z_{PDM} = \int_0^{c_*} cf(c)dc + c_* \int_{c_*}^{c_{max}} f(c)dc \qquad (9)$$

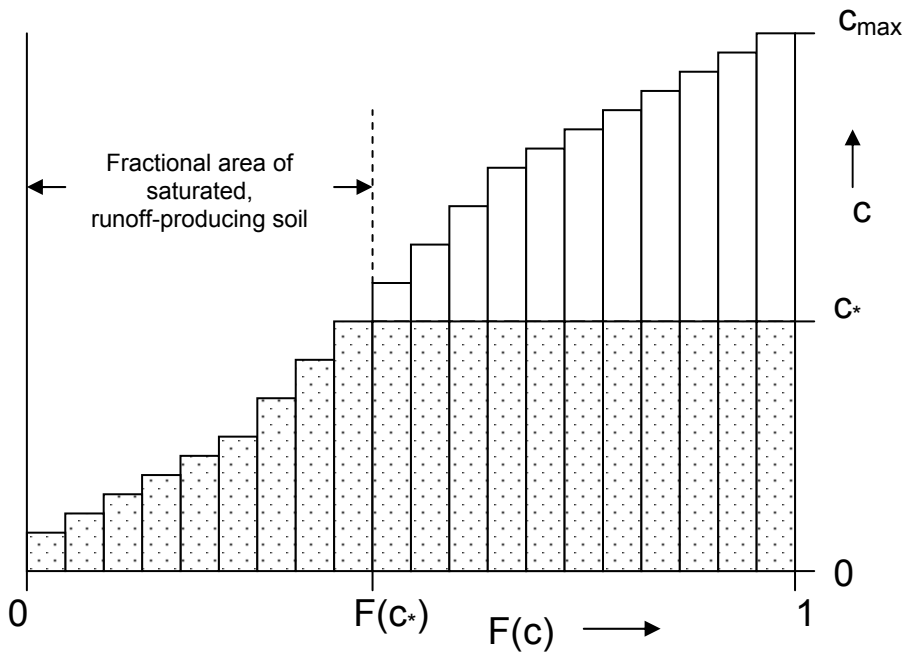

Figure 2. Schematic representation of the Probability Distributed Moisture (PDM) scheme (in discretised form for clarity). c is the local water-holding capacity of the soil, c_{max} is its maximum value and c_* is the critical value below which soils are saturated. F(c) is the fractional area of soil with capacity less than or equal to c. The stippled area represents saturated soil.

Evaluating the integrals in equation (9) and using equation (8) gives,

$$\frac{c_*}{c_{max}} = 1 - \left(1 - \frac{\theta_{PDM}}{\theta_{sat}}\right)^{1/(B+1)} \tag{10}$$

If throughfall, P_f, and/or snowmelt, S_m, is added to the soil surface during the timestep Δt (s) the critical point increases to,

$$c_*' = \min\left(c_{max}, c_* + (P_f + S_m)\Delta t\right) \tag{11}$$

The surface saturation runoff, $Y_{s(sat)}$, is then given by,

$$Y_{s(sat)} = P_f + S_m - \frac{\rho_w \Delta z_{PDM}}{\Delta t}\left(\theta_{PDM}' - \theta_{PDM}\right) \tag{12}$$

where, by using equation (10),

$$\frac{\theta_{PDM}'}{\theta_{sat}} = 1 - \left(1 - \frac{c_*'}{c_{max}}\right)^{(B+1)} \tag{13}$$

So far there has been no attempt in the Nimrod implementation of MOSES-PDM to relate the parameter B to the variability of topographic height or soil type within a gridsquare. There is also no representation of lateral gridsquare to gridsquare transports of soil moisture. Both of these are matters of ongoing research and their importance in a soil moisture diagnosis system such as the one presented here is yet to be established.

3. The implementation of MOSES-PDM in Nimrod

The analyses which Nimrod supplies for driving MOSES-PDM are now described together with their processing to form appropriate hourly accumulations and means. This section also describes the derivation of the land surface and soil parameter fields required by MOSES-PDM on the Nimrod grid and the initialisation of the MOSES-PDM prognostic fields. Figure 3 is a process diagram showing the inputs, processing components and outputs of the Nimrod implementation of MOSES-PDM.

3.1 The Nimrod precipitation amount and state analysis

The amount and state of precipitation arriving at the land surface are fundamental inputs to the MOSES-PDM soil state and surface hydrology model. If the precipitation is frozen it will augment the lying snow store in MOSES-PDM. If in the liquid state, precipitation (or any dew, melted snow and frost) may be intercepted by the vegetative canopy or fall through it to the surface. The proportion of the throughfall which runs off at the surface is calculated by the Probability Distributed Moisture (PDM) model within MOSES (as described above in Section 2.3). The remainder of the throughfall enters the top soil moisture layer. The soil state diagnosis made by MOSES-PDM in Nimrod requires the *precipitation analysis* from Nimrod. The soil state and surface hydrology calculations could easily be extended into a forecast with inputs from Nimrod's *precipitation forecast*.

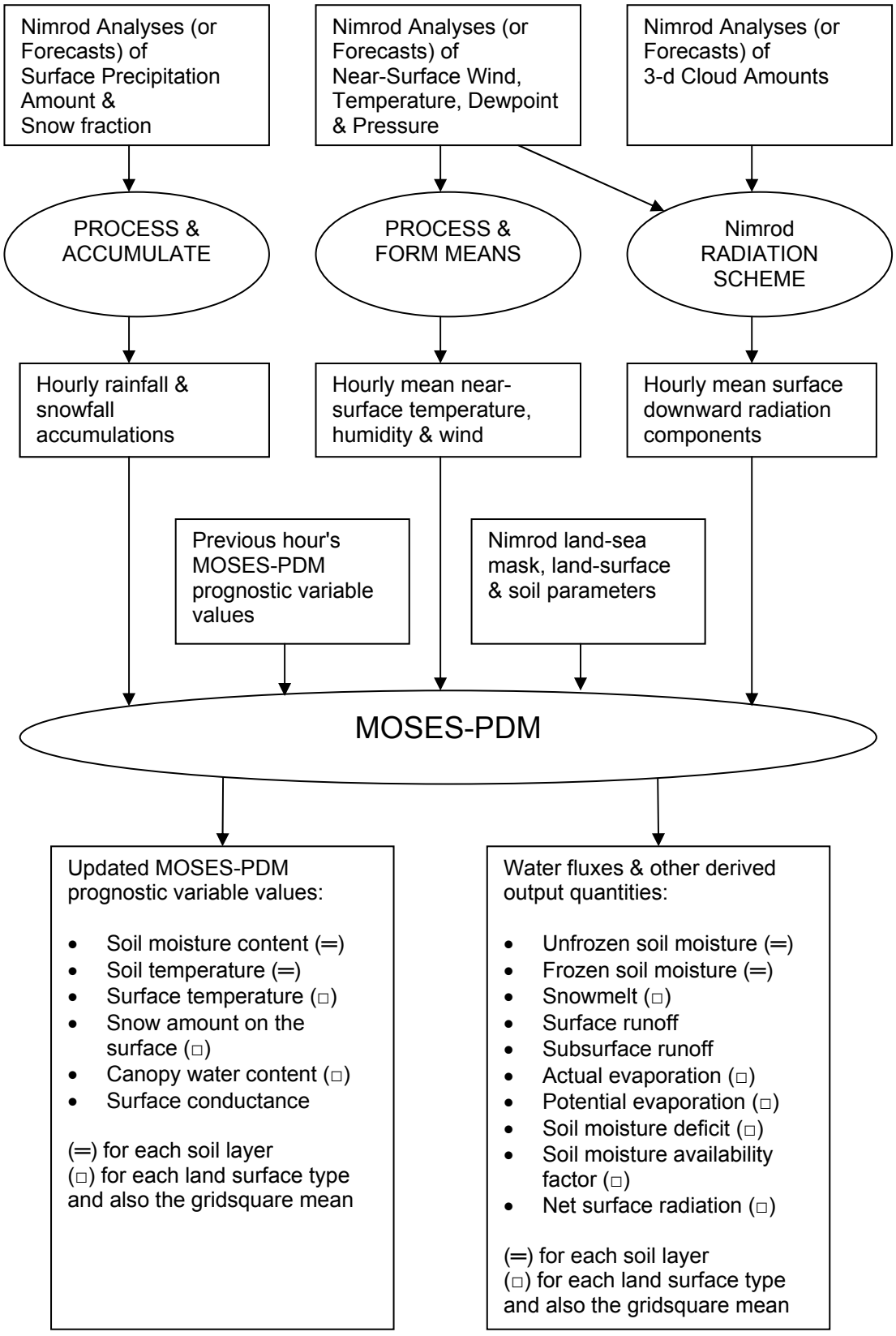

Figure 3. The inputs, outputs and processing components of Nimrod-MOSES-PDM.

Nimrod's automated processing of radar data and satellite and surface information to produce a precipitation analysis has five main components (Golding, 1998). The first four are carried out on single site radar images before a final stage of forming a composite image and combining it with other data sources. The first process identifies and removes corrupt images. Secondly, spurious echoes within an image are identified and removed using a Bayesian approach with three predictors from satellite imagery, surface synoptic reports and a precipitation forecast. This has considerable scope for calibration by adjusting thresholds for rejection. An optimum balance between removal of real echoes and retention of spurious ones has to be maintained. The third process corrects echo intensity for range, bright-band contamination and orographic enhancement below the radar beam. This is based on a physical parametrization of the reflectivity profile, calibrated with radar observations, and used to determine the surface precipitation rate. Rain gauge calibration of the radar surface precipitation intensities forms the fourth component of the processing of the individual radar site data. Correction factors are recalculated and applied on a weekly basis.

Corrected single site radar images are composited using a pre-defined preference map to form a single radar image covering Britain, Ireland and, with the recent incorporation of other countries' radar data, extension into continental Europe. In areas of the Nimrod domain beyond radar range, or where a particular radar is temporarily missing, precipitation data are derived with a variational analysis technique using satellite and surface information together with a first guess forecast. Golding (1998) describes how threshold satellite radiances are determined which maximise the skill in reproducing the radar precipitation distribution. The thresholds are applied to satellite data covering the whole domain to provide estimates of precipitation rate where radar data are unavailable.

The Nimrod precipitation rate analysis at 5km resolution is performed every 15 minutes. An accumulated precipitation amount over the 1 hour timestep used for MOSES-PDM within Nimrod is formed from five 15-minute rates with the first and last given half weighting. Thus the T-60, T-45, T-30, T-15 and T-0 minute instantaneous rates (mm hr^{-1}) are combined to give an accumulation (mm hr^{-1}) for the period from T-1 to T-0 hours.

The fraction of the hourly accumulation which is snow is estimated (Golding, 1998) for clouds in which the coldest temperature is less than -1^{o}C (otherwise zero fraction of snow is set). The vertical profile of atmospheric temperature comes from hourly NWP model data ingested in Nimrod. The height integral of positive wet bulb temperatures from ground to freezing level is calculated. The fraction of precipitation which is assumed to be snow varies linearly between zero for values of the integral exceeding 450 K m and unity for values less than 25 K m. The snow fractions for the times T-1 and T-0 hours are averaged to form the fraction applied to the accumulation for the period between these times. Thus the rain and snow accumulations for each hour are made available to MOSES-PDM.

3.2 Near surface temperature, humidity, wind and pressure

To calculate the turbulent fluxes of heat and water from the surface tiles into atmosphere, MOSES-PDM requires the temperature, humidity, wind and pressure at a reference level near the surface. Strictly the reference level should be at a "blending height" above which the atmospheric variables are no longer influenced by the individual surface tiles, just their aggregated effect. The current implementation of MOSES-PDM in Nimrod uses analyses at screen level for temperature and humidity and at 10m above the surface for wind and pressure. Future development

of Nimrod will enable analyses at blending height to be made available for turbulent flux calculations.

The screen level temperature and humidity analysis in the Nimrod system is part of its visibility analysis (Wright and Thomas, 1998). The analysis uses first-guess values of liquid water temperature, $T_l = T - (L/c_p)q_l$ and total water, $q_T = q + q_l$, where T is the temperature, q is the water vapour mixing ratio, q_l is the liquid water mixing ratio, c_p the specific heat of air at constant pressure and L is the latent heat of evaporation. The first-guess values are from a prior forecast and are modified with surface observations of temperature, dew point and visibility and a fog mask deduced from satellite imagery (Golding, 1998). The procedure simultaneously minimises the error of fit to T and q using a variational analysis method.

Wind and pressure are currently taken directly from Met Office mesoscale NWP model forecasts. Analyses of these variables incorporating surface observations have recently become available within Nimrod and it is planned to use them in the MOSES-PDM calculation of surface fluxes. Values of all the near-surface atmospheric variables are obtained in Nimrod every hour. The mean of values at T-1 and T-0 hours are used for calculating the evaporative and heat fluxes over the period T-1 to T-0 hours and thence increments for updating the prognostic soil moisture and temperature and surface snow amount from timelevel T-1 values to T-0 values.

3.3 The calculation of downward radiation components

Downward radiation fluxes are required by MOSES-PDM for its calculation of the surface energy balances for each surface tile of each grid-square. These fluxes were not available in the Nimrod system and so it was necessary to include a scheme to calculate them from other variables, notably cloud cover, that are available in Nimrod.

The Nimrod 3-dimensional cloud amount analysis

The 3-dimensional cloud distribution is a major factor in the determination of both the short-wave (solar) and long-wave downward radiation. Cloud has been analysed and forecast at hourly intervals by the Nimrod system from its operational introduction in the mid-1990's. Until the implementation of MOSES-PDM in Nimrod, the main users of the cloud products from Nimrod have been aviation, the utility and leisure industries and the general public. The Nimrod cloud analysis has a horizontal resolution of 15km and is the only input to the surface hydrology and soil state model in Nimrod which is everywhere of lower resolution than the surface scheme.

The Nimrod 3-d cloud analysis is calculated from a first-guess field of cloud amounts which is adjusted with data from radar, satellite and surface-based observations using a recursive filter analysis in each of 26 horizontal layers (Golding,1998). The first-guess field is a 1 hour Nimrod cloud amount forecast, if available, otherwise a NWP model cloud amount forecast. At present, the main remotely observed data come from Meteosat satellite imagery but improvements are anticipated from Meteosat Second Generation (MSG) products within the next year. Improved data and processing algorithms should feed through to more accurate cloud analyses. The use of radar precipitation data ensures that there is consistency between Nimrod's analysed precipitation and cloud fields. If the surface hydrology and soil state model in Nimrod were to be operated in forecast mode then Nimrod's 3-d cloud forecast (obtained by advecting analysed cloud fields) would be used.

The radiation calculations described below require Nimrod's multi-layer cloud analysis to be simplified into cloud cover fractions for low, medium and high cloud. Predefined heights above the surface are taken as the boundaries between the three

categories. The "low" category includes cloud between 100m and 2000m, "medium" between 2000m and 8000m and "high" between 8000m and 25000m. For these three layers, the cloud fractions are computed using the maximum fraction from the model layers within them.

Radiation scheme inputs

Downward long-wave radiation is calculated using the high, medium and low cloud fractions together with the fields of surface air temperature and vapour pressure. Solar radiation is calculated from the solar radiation at the top of the atmosphere attenuated by an amount determined by clouds and atmospheric turbidity due to aerosols. The solar radiation at the top of the atmosphere is determined from astronomical formulae requiring time, latitude and longitude inputs. Cloud fractions and surface temperature and humidity are taken to be the mean of the values calculated at the beginning and end of each 1-hour timestep used for MOSES-PDM within the Nimrod system.

Downward long-wave radiation

The downward long-wave radiation flux density at the Earth's surface, R_L (W m^{-2}), from the atmosphere is calculated using the Stefan-Boltzmann relationship,

$$R_L = \varepsilon\sigma T_a^4 \qquad (14)$$

where σ is the Stefan-Boltzmann constant (5.67×10^{-8} W m^{-2} K^{-4}), ε is an appropriate emissivity, and T_a is the air temperature (K). The emissivity is the product ($\varepsilon = \varepsilon_a K$) of the effective emissivity, ε_a, of a clear atmosphere, and an enhancement factor K that represents the effect of clouds. ε_a is calculated using the formula of Brutsaert (1975) which gives,

$$\varepsilon_a = 1.24\left(\frac{e}{T_a}\right)^{1/7} \qquad (15)$$

where e is the vapour pressure (mbar). The enhancement of the clear-sky emissivity by clouds is calculated using fractional cloud cover in the three categories, low, medium and high. A random combination of the three cloud layers is used to determine, K so that,

$$K = 1 + k_L c_L + (1 - c_L)\left[k_M c_M + (1 - c_M) k_H c_H\right] \qquad (16)$$

where c and k are the fractional cloud cover and cloud type parameter respectively for low, medium and high cloud denoted by the subscripts L, M and H respectively. The values of k_L = 0.21, k_M = 0.16, and k_H = 0.06, are based on those of Arnfield (1979). Equation (16) ensures that the effects of the lowest clouds present are dominant.

Downward solar radiation

The solar radiation flux density at a point on the Earth's surface, R_S (W m^{-2}), is calculated from,

$$R_S = \tau_a \tau_c R_A \qquad (17)$$

where R_A (W m^{-2}), is the radiation at the top of the atmosphere, τ_a is the clear-sky transmittance and τ_c is the cloud transmittance allowing for attenuation through absorption and scattering.
The solar radiation at the top of the atmosphere for a specific time period and specific location is calculated using,

$$R_A = \frac{12}{\pi} S_0 s_s \left[\sin(\varphi in(\varphi)\delta)\Delta_t + \cos(\varphi os(\varphi)\delta)\Delta_s\right] \quad (18)$$

following Allen *et al*., (1994). S_0 (1367 W m^{-2}), is the solar constant, s_s, is the (dimensionless) solar scaling constant that allows for the changing distance between the Sun and the Earth, φ is the latitude and δ the solar declination, both in radians. Δ_t is the difference between the solar time angle at the beginning and end of the period and Δ_s is the difference between the sines of these angles. The periods considered are the 1-hour timesteps for updating the soil and surface variables.
The clear-sky transmittance is calculated as the sum of two parameters a and b that vary with location, and with location and season, respectively. The values for these parameters are taken from tables derived for the MORECS (Thompson *et al*., 1981). It is therefore necessary to determine the appropriate MORECS grid square containing the Nimrod grid-square. Nimrod grid-squares outside the MORECS area are simply assigned the mean value for each of the parameters.
The total cloud transmittance factor is calculated by using a random combination of the transmittances of the three cloud layers thus,

$$\tau_c = \left[1-(1-T_H)c_H\right]\left[1-(1-T_M)c_M\right]\left[1-(1-T_L)c_L\right] \quad (19)$$

where the subscripts H, M and L denote high, medium and low cloud respectively and where the transmittance of the cloud layers ($T_{L,M,H}$) is calculated from (Haurwitz, 1948),

$$T_{L,M,H} = k_1 \exp(-k_2 m_\tau) \quad (20)$$

The values of k_1 and k_2 for the different cloud types are given in Table 1, and the optical air mass (m_τ) traversed by the solar radiation is calculated following Kasten (1966) from,

$$m_\tau = \left[\sin(\gamma_0\, \pi/180) + 0.15(\gamma_0 + 3.885)^{-1.253}\right]^{-1} \quad (21)$$

where γ_0 is the solar elevation in degrees.

Table 1. The cloud transmittance parameters derived from values given in Haurwitz (1948)

cloud level	k_1	k_2
low	0.8967	0.0545
medium	0.4846	0.0285
high	0.3461	0.037

The fraction of the timestep during which there is sunshine, S_f, defined as clear sky conditions, is also output from the scheme, but not used in any other calculations, using,

$$S_f = F_s(1-c_L)(1-c_M)(1-c_H) \quad (22)$$

where F_S is the fraction of the time step when the Sun is above the horizon.

3.4 The derivation of land use fields

MOSES-PDM requires ancillary fields specifying the fractional coverage of each land surface type within each Nimrod grid-square. In reality these fractions change by direct and indirect effects of human actions or because of natural climate variations. However, for this implementation of MOSES-PDM in the Nimrod system they have been pre-calculated and are kept constant in time.

The 25m resolution Land Cover Map of Great Britain (Fuller *et al.,* 1994) was used to provide data for Nimrod grid-squares within Great Britain. Elsewhere, version 1.2 of the 1km resolution IGBP Global Land Cover Characteristics Database (Loveland *et al.*, 2000) was used. The Land Cover Map of Great Britain is based upon LANDSAT TM data for 1995 and the IGBP database is derived from 1km resolution AVHRR 10-day composites for April 1992 through March 1993.

The first step in creating the Nimrod ancillary land use fields was to create a map of tile fractions based upon the IGBP data. The land cover data was not interpolated onto the Nimrod grid, instead pixels were assigned to the Nimrod grid-square which contains their centre. In order to convert from the IGBP classification to the MOSES-PDM tile type the mapping shown in Table 2 was used. In this way for each Nimrod grid-square the total number of pixels and hence the fractional coverage of each tile type can be determined. This process was repeated using the Land Cover Map of Great Britain and the mapping described in Table 3.

The map of fractional land use cover derived from the IGBP data was used to generate a land-sea mask. All Nimrod grid-squares which were more than fifty percent water were classified as sea points, everything else was assumed to be land. However since the IGBP land cover classifications do not distinguish between sea and inland water, the resulting land-sea mask was converted to a bitmap and edited by hand.

Finally a composite of the two land cover maps was created. All points classed as sea points in the land sea mask were flagged as missing data. For those land points where the Land Cover Map of Great Britain data is available it was preferred, elsewhere IGBP data was used. The result of the process just described is a set of ten ancillary files each containing the fractional coverage of one of the MOSES-PDM tile types for every grid-square in the Nimrod domain.

MOSES-PDM tile type	IGBP classification
Broad-leafed tree	• Evergreen broadleaf forest • Deciduous broadleaf forest • 0.5 * Mixed forest
Needle-leafed tree	• Evergreen needle-leaf forest • Deciduous needle-leaf forest • 0.5 * Mixed forest
C3 Grass	• Savannah • Grasslands • Permanent wetlands • Cropland / natural vegetation mosaic
C4 Grass	-
Crop	• Croplands
Shrubs	• Closed shrublands • Open shrublands
Urban	• Urban & built up
Inland water	• Water
Bare soil	• Barren and sparsely vegetated
Ice	• Snow and ice

Table 2. Mapping of IGBP land cover classifications to MOSES-PDM tile types.

MOSES-PDM tile type	Land cover map of GB classification
Broad-leafed trees	• Deciduous scrub and orchards • Deciduous broad-leafed and mixed woodlands.
Needle-leafed trees	• Conifer and broad-leafed evergreen trees.
C3 grass	• Semi-natural, mostly acid, grasslands of dunes, heaths and lowland-upland margins Pastures and amenity swards, mown or grazed, to form a turf throughout the growing season. • Meadows, verges, low intensity amenity grasslands and semi-natural cropped swards, not maintained as a short turf. • Lowland marsh/rough grasslands, mostly uncropped and unmanaged, forming grass and herbaceous communities, of mostly perennial species, with high winter-litter content. • Mountain/hill grasslands, mostly unenclosed Nardus/Molinia moorland. • Bracken-dominated herbaceous communities. • Upland herbaceous wetlands with permanent or temporary standing water • Ruderal weeds colonising natural and man-made bare ground • Felled forest, with ruderal weeds and rough grass. • Lowland herbaceous wetlands with permanent or temporary standing water.
C4 grass	-
Crop	• Arable and other seasonally or temporarily bare ground.
Shrubs	• Upland, dwarf shrub/grass moorland. • Upland evergreen dwarf shrub-dominated moorland. • Lowland evergreen shrub-dominated heathland. • Lowland, dwarf shrub/grass heathland.
Urban	• Suburban and rural developed land comprising buildings and/or roads but with some cover of permanent vegetation. • Industrial, urban and any other developments, lacking permanent vegetation.
Inland water	• Inter-tidal seaweed beds and salt marshes up to normal levels of high water spring tides. • Inland fresh waters and estuarine waters above the first bridging point or barrier.
Bare soil	• Bare coastal mud, silt, sand, shingle and rock, including coastal accretion and erosion features above high water. • Ground bare of vegetation, surfaced with 'natural' materials.
Ice	-
Missing data	• Sea, coastal waters and estuaries inland to the first bridging point or barrier.

Table 3. Mapping of Land Cover Map of GB classifications to MOSES-PDM tile types.

3.5 The derivation of the fields of soil parameters

The soil hydraulics and thermodynamics component of MOSES-PDM requires values for parameters (Table 4) that govern the hydrological and thermal processes in the soil.

Parameter	Name (units)
Ψ_{sat}	Saturated soil water suction (m)
K_{sat}	Saturated hydraulic conductivity (kg m^{-2} s^{-1})
b	Clapp-Hornberger exponent (-)
C_s	Dry soil volumetric heat capacity (J m^{-3} K^{-1})
λ_{dry}	Dry soil thermal conductivity (W m^{-1} K^{-1})
θ_{sat}	Volumetric soil water concentration at saturation ($m^3_{(water)}$ $m^{-3}_{(soil)}$)
θ_{crit}	Volumetric soil water concentration at the critical point ($m^3_{(water)}$ $m^{-3}_{(soil)}$)
θ_{wilt}	Volumetric soil water concentration at the wilting point ($m^3_{(water)}$ $m^{-3}_{(soil)}$)
θ_{fc}	Volumetric soil water concentration at the field capacity ($m^3_{(water)}$ $m^{-3}_{(soil)}$)

Table 4. Soil parameters required by MOSES-PDM

The first three parameters in Table 4 control the movement of water between the soil layers and out of the bottom layer. They are used in the calculation of the drainage and suction via the Darcy-Richards equation (Cox *et al*., 1999). The fourth and fifth parameters are used to calculate the temperature changes of the soil layers and the heat fluxes between them. (Cox *et al*., 1999) The saturated soil water concentration primarily controls the saturation surface runoff as described in Section 2.3. The critical point and wilting point values for the soil moisture concentration control the soil moisture stress on the evapotranspiration (Cox *et al.*, 1999). The field capacity is not used in the MOSES-PDM calculations but is required for diagnosing the soil moisture deficit (SMD) from the soil moisture amounts calculated by MOSES-PDM (see section 4 for further details of SMD and the method of derivation of the field capacity parameter).

An ancillary file was created for each parameter giving its value at each of the land grid-squares in the Nimrod domain, except for those squares which were specified as having fractional land-use of inland water or ice equal to unity (note that the ice fraction is either zero or unity). The IGBP soils database (Global Soil Data Task Group, 2000) holds, for most of the globe, the soil type specified as percentages of the constituent soil units at a resolution of 5 minutes. The parameter values, with the exception of λ_{dry} and θ_{fc}, were derived from this database which holds pedon attributes, including the four van Genuchten parameters (van Genuchten, 1980), for 106 soil units.

The procedure used to derive the parameters was as follows:

1. Calculate the Clapp-Hornberger parameters required by MOSES-PDM from the van Genuchten parameters for each of the 106 soil units, using the method of Lenhard *et al.* (1989);
2. For each Nimrod grid-square determine the nearest IGBP grid-square and retrieve the fractional coverage of the constituent soil units.
3. Use the fractional coverages to calculate appropriately aggregated grid-square parameter values representative of the soil composition, from the IGBP hydraulic and thermal parameter values for each Nimrod grid-square;

4. Write an ancillary file containing values across the Nimrod domain for each of the parameters.

With the exception of K_{sat}, the parameter values for each grid-square were calculated as areal averages using the fractional coverages of the different soil types as weightings. So, for the grid-square average parameter, $\overline{p}$,

$$\overline{p} = \sum_{i=1}^{i=s} f_i p_i \tag{23}$$

where f_i is the fractional coverage of soil type i having the parameter value p_i, and the summation is over the s soil types represented in the gridsquare.

The true gridsquare average hydraulic conductivity, $\overline{K}$, is given from equation (3) by,

$$\overline{K} = K_{sat} \overline{\left(\frac{\theta}{\theta_{sat}} \right)^{2b+3}} \tag{24}$$

where θ is the unfrozen soil moisture volumetric concentration ($m^3_{(water)}$ $m^{-3}_{(soil)}$) and the overbar denotes averaging over the gridsquare. However, sub-grid variability in the model is not known and so,

$$\overline{K} = K_{sat} \left(\frac{\theta}{\overline{\theta}_{sat}} \right)^{2\overline{b}+3} \tag{25}$$

is used, where $\overline{b}$ and $\overline{\theta}_{sat}$ are calculated using equation (23). Non-linearity results in poor agreement between equations (24) and (25) when there is a broad distribution of soil hydraulic properties across the grid-square. To improve upon this, an effective value of $K_{sat} = K'_{sat}$ is calculated, which gives the correct value of $\overline{K}$ when $\theta/\theta_{sat} = 0.5$, from,

$$K'_{sat} = \overline{K}_{sat} 0.5^{-\left(2\overline{b}+3\right)} \tag{26}$$

where $\overline{K}_{sat}$ is calculated from

$$\overline{K}_{sat} = \sum_{i=1}^{s} f_i K_{sat,i} 0.5^{2b_i+3} \tag{27}$$

An attempt to apply the method of Hubrechts and Feyen (1996) for deriving the dry soil thermal conductivity, λ_{dry}, from the IGBP soil composition data proved to be unsuccessful. The suggested algorithm produced singularities for some gridsquares. A uniform value for λ_{dry} of 0.239 W m^{-1} K^{-1} was therefore set for the whole Nimrod domain (cf. the range 0.218 to 0.272 W m^{-1} K^{-1} for λ_{dry}, derived from the Wilson and Henderson-Sellers (1985) dataset, in the version of MOSES implemented in the Met Office Unified NWP and General Circulation Model (Cox *et al*., 1999).)

Because of the different grids used in the IGBP data base and Nimrod domain, not all Nimrod grid-squares with surface types having soil, had corresponding IGBP squares. The missing parameter values were filled in using the values from the majority of the surrounding Nimrod grid-squares. If the immediately adjacent squares also contained missing values then the range was extended outwards as necessary.

3.6 The initialisation of prognostic variables in MOSES-PDM

The variable fields in MOSES-PDM which are updated each timestep, the "prognostic variables", include the soil moisture and temperature for each of the four soil layers, the surface temperature, amount of lying snow and canopy water content for each surface type present within a gridsquare. They each need to be assigned initial values whenever the model starts without the previous hour's values being available. Normally the model calculates updated prognostic fields from those stored from the previous hour using the mean fluxes of water and energy over the hour. However, when the model is run for the very first time or if a computer software or system failure results in one or more missed hourly runs of the model, there must be a way of assigning sensible values to the prognostics so that update calculations can proceed.

The procedure adopted in this implementation of MOSES-PDM within the Nimrod nowcasting system is to look for the previous hour's (T-1) values of each prognostic variable field in turn (all variable Nimrod fields contain a yyyymmddhhmm date/time-stamp in their names). If it is not found then the field for the hour before (T-2) is sought and so on until a value (T-n) is found to be present. The value found is then taken as the T-1 value. If a field has not been found with a date/time-stamp within the previous 24 hours then an NWP forecast field is sought with a validity time of T-1 and the shortest available lead time for the field in question. The field from the NWP model will have been interpolated to the finer Nimrod grid but obviously lacks the resolution of the Nimrod fields.

It could be argued that an NWP model field with the appropriate (T-1) validity time should be preferred to an "old" (T-n, $2 \leq n \leq 24$) Nimrod-MOSES-PDM field. However, for quantities with a long memory and spin-up time like soil moisture, soil temperature at depth and the amount of lying snow it has been judged preferable to re-initialise, if necessary, from an old Nimrod field, even though it hasn't "seen" the rainfall, evaporation etc. for the period T-n to T-1, rather than to lose the high resolution detail in the Nimrod field by using a NWP model field.

During the initial trial period when some model coding errors caused failures, the procedures for re-initialisation from old Nimrod or NWP fields were invoked fairly frequently. However, after correction of all detected code errors, the Nimrod implementation of MOSES-PDM has run without failure for over six months. Occasional problems with the Nimrod system (unrelated to the MOSES-PDM model) can sometimes cause a few hourly runs to be missed. In these circumstances the automated search for and use of "old" Nimrod fields has enabled the sequence of hourly MOSES-PDM runs to restart without human intervention.

3.7 The time variation of vegetation physiological characteristics

The Leaf Area Index (LAI) for each vegetation type is required by MOSES-PDM for calculating the canopy conductance, the area of bare soil exposed beneath the vegetation and the maximum water holding capacity of the vegetative canopy. The root depth for each vegetation type is required for calculating the vertical profile of evaporative extraction from the soil layers (Cox *et al*., 1999; Essery *et al*., 2003). Canopy height for each vegetation type is required for calculating the canopy conductance and heat capacity.

For the MOSES-PDM land use type "crops" the annual variation of LAI, root depth and canopy height are specified to be those respectively assumed in the MORECS "spring barley" crop type (Hough and Jones, 1997). For MOSES-PDM land use type "deciduous tree" only the LAI has an imposed annual variation, again to match that of MORECS. For all other vegetation types constant values of LAI, root depth and canopy height are assumed, again matching those in MORECS.

4. Quantities calculated and output by the model

The purpose of running MOSES-PDM within the Nimrod system is to produce surface and sub-surface hydro-meteorological outputs useful to a range of customers. All Nimrod fields are calculated and output on a grid of whatever resolution is chosen (currently 5km). For many customers aggregations of quantities over time and/or space may be more useful. Nimrod itself does not provide a comprehensive aggregation and display facility using a Geographical Information System (GIS) to overlay, for example, river catchment boundaries. However, GIS-based display and processing systems are under development which accept gridded fields from Nimrod or NWP models as inputs. These could be run either in-house in the Met Office or by customers receiving automated data transfer from the Nimrod system.

4.1 Prognostic variables and water fluxes

The primary outputs from MOSES-PDM are hourly updates of its prognostic state variables. These are the time-varying quantities, internal to MOSES-PDM, whose values are required at the beginning of a timestep for the calculations to proceed. The latest values of MOSES-PDM's prognostic variables are potentially useful to customers as well as being essential for the next hourly run of the model. They are the soil moisture for each of the model's soil layers, the soil temperature for each of the soil layers, the surface temperature of each land-type, the amount of snow lying on each land-surface type, the water held in the vegetative canopy for each land-surface type and the conductance for calculating the evaporation from the surface (Cox *et al*., 1999). For each of the variables which are "tiled", i.e. calculated for each of the land-surface types within a gridsquare (Essery *et al*., 2003), a gridsquare mean is calculated for output by using the fractions of the respective land-surface types as weighting factors in the sum over types.

An example of a prognostic quantity output by Nimrod-MOSES-PDM can be seen in Figure 4(a). This shows a timeseries of the daily mean values of the sum of the top three soil layers' soil moisture, i.e. the moisture in the top 1 metre of soil, divided by the value at saturation, $(M_1+M_2+M_3)/(M_{1(sat)}+M_{2(sat)}+M_{3(sat)})$, for a gridsquare in southern England (centre of square at latitude 52.07 degrees north and longitude 1.45 degrees west) over the period March to September 2003. The drying out of the soil during the spring and summer period is evident with wetting events matching the precipitation (Figure 4(b)).

The second class of outputs provided for users from the Nimrod implementation of MOSES-PDM are the fluxes of water and energy which are calculated within MOSES-PDM during each timestep for the respective budgets and prognostic equations. Into this category of derived quantities fall the surface runoff, subsurface runoff (i.e. drainage from the bottom of the lowest soil layer), snowmelt for each land-surface type, actual evaporation from each land-surface type and the net surface radiation for each land surface type (short-wave and long-wave components as well as the total). Again tiled quantities are aggregated to form gridsquare means for output. Figure 4(b) shows examples of water fluxes output by Nimrod-MOSES-PDM. Here the daily accumulations of surface runoff along with the analysed rainfall (both in mm day^{-1}) for a gridsquare in southern England are plotted as a timeseries for the period March-September 2003. The runoff is a fairly small proportion of the precipitation during this period with dry soil. Figure 4(c) shows the timeseries of the gridsquare mean actual evaporation (AE), together with the potential evaporation

(PE) (see Section 4.3 below) for the same gridsquare. Early in the period the AE is close to its potential value but as the soil dries out in the late spring and summer the AE becomes significantly less than the PE. Both AE and PE show increase in the spring and decrease in the early autumn because of the annual variation of solar radiation.

Maps of the accumulated rainfall (mm hr^{-1}), surface runoff (mm hr^{-1}), gridsquare mean AE and PE (mm hr^{-1}x695 ≈ W m^{-2} latent heat) for the hour 14:00-15:00 GMT on 20 September 2003 from Nimrod-MOSES-PDM are shown in Figures 5(a), (b), (c) and (d) respectively. The Nimrod precipitation analysis shows a rainband of moderate intensity lying across northern England, the northernmost parts of Wales and south-east Ireland as well as showers over Scotland. The potential evaporation calculated by MOSES-PDM is lower in areas covered by the rainband because the associated cloud reduces the solar heating at the surface (see Figure 6(b)). The actual evaporation is considerably lower than the potential evaporation over much of England, Wales, France and Germany because of the dryness of the soil at the end of the summer.

The runoff, either in its raw gridded form or aggregated over catchments, could be input to flow routing models (Fread, 1985; Bell and Moore, 1998) to calculate river flow and extent of any flooding. River flows are measured quite extensively in many countries by agencies responsible for river management and flood warning. There are nevertheless ungauged rivers in remoter areas or less economically developed countries. It is planned to couple flow routing models with MOSES-PDM. For gauged rivers this would provide a method for evaluation of the whole rainfall-runoff-flow calculation system using observed flows. For ungauged rivers the outputs would be useful for giving flood warnings. Including routing of runoff from MOSES-PDM would extend the capability of the Nimrod nowcast system or of an NWP or climate modelling system incorporating MOSES-PDM as its land-surface processes component. Work towards this end has been done with other NWP models and land surface schemes for short and medium range forecasts by Yu *et al*. (1999) and De Roo *et al*. (2003), and for climate simulation purposes by Oki *et al*. (2001), Sausen *et al*. (1994) and Miller *et al*. (1994).

A third class of quantities are derived from MOSES-PDM within Nimrod and are output because they are particularly useful to customers. These include potential evaporation, the soil moisture deficit and soil moisture availability factor for each land-surface type.

4.2 The soil moisture availability factor

The soil moisture availability factor for soil layer k, β_k, which is used in the MOSES-PDM calculation of actual evapotranspiration, is defined as:

$$\beta_k = \frac{\theta_{(u)k} - \theta_{wilt}}{\theta_{crit} - \theta_{wilt}} \qquad (28)$$

with a maximum value of unity and a minimum value of zero, where $\theta_{(u)k}$ is the volumetric unfrozen soil moisture concentration of layer k, θ_{wilt} is the volumetric soil moisture concentration at wilting point and θ_{crit} is the volumetric soil moisture concentration at the critical point. (See Section 3.5 for definitions and units of soil parameters.) To find the overall availability factor for each vegetated land-surface type t, β_t, the values for each soil layer are summed with root fraction weighting factors,

$$\beta_t = \sum_{k=1}^{nsoil} r_{t,k}\beta_k \qquad (29)$$

where nsoil is the number of soil layers and $r_{t,k}$ is the proportion of the plant roots in soil layer k for surface type t. $r_{t,k}$ is defined in terms of the root depth, $R_{D,t}$ for vegetated surface type t by assuming an exponential root profile (Thornley and Johnson, 1990) so that,

$$r_{t,k} = \frac{e^{-pz_{k-1/2}/R_{D,t}} - e^{-pz_{k+1/2}/R_{D,t}}}{1 - e^{-pz_{nsoil+1/2}/R_{D,t}}} \qquad (30)$$

where p =2 and $z_{k+1/2}$ is the depth of the bottom of soil layer k ($z_{1/2} = 0$).

For each of the vegetated surface types, β_t multiplies the stomatal conductance and net leaf photosynthesis in MOSES-PDM (Cox *et al*., 1998). For output only, values of the availability factor are also set for the non-vegetated land-surface types (urban, inland water, bare soil and ice): β_t is set to unity for inland water and ice and to the top soil layer value for urban and bare soil. A gridsquare mean value of β is calculated for output by weighting each β_t with the corresponding land-use fraction and then summing over all surface types.

4.3 Potential evaporation

Many potential customers for Nimrod's surface hydro-meteorological products have expressed the need to use potential evaporation as an input for their own hydrological models. This quantity has therefore been added to the outputs of MOSES-PDM. It is calculated in the same way as the actual evaporation each timestep except that the soil moisture availability factor is set to unity. Thus it represents the evaporation as it would be if there was no evaporative stress due to sub-critical soil moisture. It should be noted that potential evaporation is calculated only for output - it is the actual evaporation which enters the MOSES-PDM energy and water budgets.

An example of a field of gridsquare mean potential evaporation produced by Nimrod-MOSES-PDM is shown in Figure 5(d) for the hour 14:00-15:00 on 20 September 2003. The values in mm hr^{-1} have been multiplied by 695 so that they can be stored as integers in the Nimrod system without loss of significant accuracy and are displayed multiplied by this factor in the figure. The factor 695 was chosen since it turns the evaporation into a latent heat in W m^{-2}.

4.4 Soil moisture deficit

MORECS (Hough and Jones, 1997), which the Met Office and its customers have relied upon for hydro-meteorological products for over twenty years, calculates soil moisture deficit (SMD), i.e. the amount of water which would be required to bring the soil to its field capacity, as its basic prognostic variable. Many potential customers for Nimrod-MOSES-PDM products still require this quantity. Since the formulation of MOSES-PDM does not involve the concepts of field capacity or soil moisture deficit, extra calculations have been added to estimate SMD from the soil moisture content in MOSES-PDM.

The SMD calculation adopted for operational use in the Nimrod implementation of MOSES-PDM differs in several ways from that described by Blyth (2002). MORECS calculates SMD for soils with high (90 percentile), median (50 percentile) and low (10 percentile) available water capacity (Hough and Jones, 1997). In order to

produce approximately equivalent products from MOSES-PDM's soil moisture content variable, the concepts and formalism which form the basis of PDM's treatment of soil heterogeneity are exploited.

The soil moisture concentrations for high, median and low water holding capacity soils are given by,

$$\frac{\theta_{high}}{\theta_{sat}} = \min\left(\frac{c_*}{c_{0.6}},1\right) \tag{31}$$

$$\frac{\theta_{median}}{\theta_{sat}} = \min\left(\frac{c_*}{c_{0.5}},1\right) \tag{32}$$

$$\frac{\theta_{low}}{\theta_{sat}} = \min\left(\frac{c_*}{c_{0.4}},1\right) \tag{33}$$

where c_* is the critical value of the storage capacity below which stores are full (see Section 2.3, particularly equation (10)) and c_{WI}, for WI = 0.6, 0.5, 0.4, is the largest value of storage capacity in the Wetness Index area, given by,

$$\frac{c_{WI}}{c_{max}} = 1-(1-WI)^{1/B} \tag{34}$$

c_{WI} is the value of c when F(c), given by equation (6), is set to the Wetness Index, WI. Equations (31)-(33) express the assumption that when the WI capacity, c_{WI}, exceeds the critical capacity, c_*, the soil moisture concentration corresponding to WI, as a fraction of its saturated value, is equal to the fraction of the WI capacity that is saturated (see Figure 7). The WI values 0.6 and 0.4 strictly correspond to 60 percentile and 40 percentile values respectively of the distribution function and were chosen so as to bring the derived high and low capacity soil moisture deficits close to MORECS' 90 percentile and 10 percentile values.

The soil moisture concentrations in each layer are then converted into deficits for each vegetated surface type t by summing layer deficits over the soil layers with root fraction profile values as weighting factors:

$$SMD_t = R_{D(max),t}\sum_{k=1}^{nsoil} r_{(max)t,k}\max\left(0,(\theta_{fc}-\theta_k)\rho_w\right) \tag{35}$$

This calculation is performed for each of the high, median and low soil capacity values of θ_k. θ_{fc} is the field capacity set using the method described below. Note that for calculating SMDs the maximum value of the root depth over the annual cycle is used, both directly as the leading factor and in the calculation of the root fraction profile. A varying root depth would cause SMD to vary even if there was no rainfall, evaporative extraction or drainage. SMD is set for non-vegetated surface types as follows: SMD is set to zero for inland water and ice and the SMD is set to the top soil layer value for bare soil and urban. Finally gridsquare mean SMDs for high, medium and low capacity soils are calculated by summing over all land-surface types weighting with land-use fraction. The SMD for a median soil for a gridsquare in southern England for March-September 2003 is shown in Figure 4(d). Figure 6(a)

shows a map of the SMD for a median soil from Nimrod-MOSES-PDM at 15:00 GMT on 20 September 2003.

The field capacity, which provides the reference value to calculate deficits from soil moisture, is not a soil parameter used in MOSES-PDM. The values used for calculating SMD in the formula above have been derived empirically from the soil hydraulics component of MOSES-PDM itself, run off-line as follows. The soil moisture content was initialised to 0.8 of its saturated value for all land points in the Nimrod domain and the model soil was allowed to drain with hourly timesteps and zero increments from rainfall and evaporation. Price (1996), states that real soils can be said to be at field capacity after 2-5 days of this pure drainage process. However, for all but the areas with the largest hydraulic conductivity, the soils as modelled in MOSES took much longer than this to reach a state of small residual drainage. The values of the soil moisture (averaged over the top three model layers) after 30 days of drainage were taken to be the field capacity values.

There are several stages in the derivation of SMD described above where pragmatic empiricism has been applied: in the choice of the percentile values chosen for the PDM distribution function to mimic MORECS' 90 percentile and 10 percentile soils (equations 31 and 33), in the root density weighting of the model soil layers (equation 35) and in the choice of starting value and drainage time of the off-line field capacity calculation. It must be stressed once again that none of this changes how MOSES-PDM does its calculations and updates its prognostic variables. MOSES-PDM doesn't use the derived SMD or field capacity in any way. The empirical approach is justified as a way of producing specific outputs for customers who are used to receiving certain hydro-meteorological products from the differently formulated MORECS. A comparison study is underway, and will be reported elsewhere, between MOSES-PDM and MORECS outputs when both are driven by historical meteorological data over a period of 40 years.

As well as the different prognostic soil variables in MOSES-PDM and MORECS, the other major difference between the two models is that MORECS calculates a separate sub-surface water balance for each of its land surface types. The tiles in MOSES-PDM do not extend below the surface and so there is only one gridsquare mean soil moisture value in each layer. MOSES-PDM could be run repeatedly in single-tile mode for each surface type to produce separate sub-surface water balances if the users' benefits justified the extra computational cost.

4.5 Verification

A comprehensive verification of outputs from Nimrod-MOSES-PDM is not easily done. In situ measurements of soil moisture profiles are sparse and, because of soil heterogeneity, they are rarely representative of a gridsquare. Blyth (2002) reports a comparative verification of MOSES-PDM and MORECS against in situ soil moisture measurements. It should be noted that Blyth (2002) ran both models "off-line" for the two sites in this study, i.e. not in the operational Nimrod context described in this paper but rather driven with site-specific observed meteorological data. Blyth (2002) found that, for a grassland site, the winter to summer range of the soil moisture simulated by MORECS was too low and MORECS' underestimation of the drying of the soil led to its wetting in the autumn occurring too quickly. The soil moisture simulated by MOSES-PDM in Blyth's (2002) study followed the observed annual cycle more closely. Further validation of MOSES-PDM is planned using data from field experiments in British lowland catchments.

Soil moisture derived from remotely sensed data (Burke and Simmonds, 2001a) have greater validity for an extended area such as a Nimrod gridsquare. However, satellite

data can only tell us about the top few centimetres of soil and allowance has to made for any vegetation cover. Attempts have nevertheless been made to use remotely sensed data with soil state models similar to MOSES-PDM (Burke and Simmonds, 2001b). It is hoped that remotely sensed microwave brightnesses can be used along with in situ data from field experiments to validate MOSES-PDM in future studies.

The runoff produced on the Nimrod grid could also be input to river routing models and the resulting flow verified against observations. This would verify the complete Nimrod-MOSES-PDM-routing model system but any errors could be difficult to trace to a specific component of the system. It is planned to conduct such a verification when a routing model has been incorporated in the Nimrod system.

The accuracy of the soil moisture and runoff from Nimrod-MOSES-PDM will depend not only on the formulation of the model but also on the analyses of meteorological variables used to drive it. The Nimrod analyses usually combine data from all available sources and so their routine validation against independent data is not possible. However, the analyses of precipitation currently produced by Nimrod do not include rain gauge data. This is because, until very recently, gauge data have not been available in sufficient quantity in real-time for combination with remotely sensed data. The accuracy of quantitative estimates of precipitation derived from radar has therefore been possible by comparison with gauge data. The trend to greater accuracy of precipitation estimates from radar has been presented by Kitchen and Harrison (2001). Planned changes to radar data processing, particularly in those localised areas subject to persistent bias errors due to occultation (beam blockage), should further improve the accuracy of Nimrod's quantitative estimates of precipitation from radar. The Met Office, through collaboration with the Environment Agency, has recently been able to receive a sufficient number of rain gauge reports from England and Wales to allow hourly analyses to be calculated in real-time by combining gauge and radar data using the statistical method of "kriging with external drift" (described in Goovaerts, 1997). When these analyses become available as operational products in the Nimrod system they should provide further improvements to the accuracy of the hourly accumulations of precipitation input to MOSES-PDM.

Figure 4. Timeseries of some daily mean outputs from Nimrod-MOSES-PDM for a gridsquare in southern England (latitude 52.07 degrees north and longitude 1.45 degrees west).

(a) Soil moisture in top metre of soil (fraction of saturation)

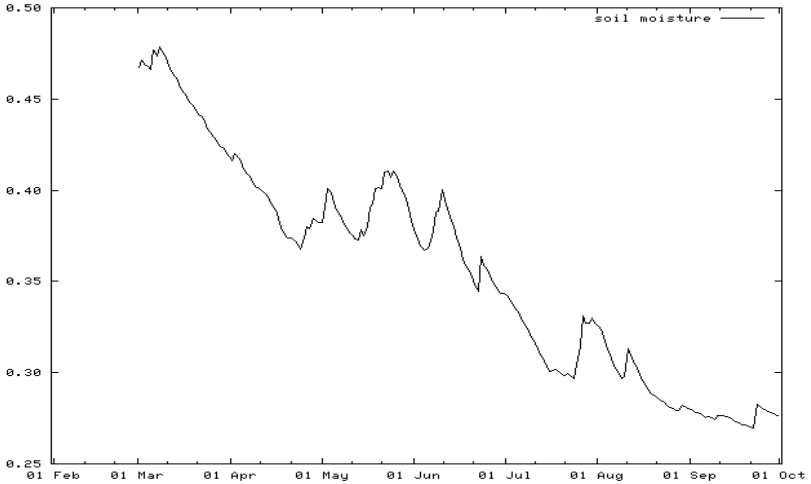

(b) Rainfall and surface runoff (mm day^{-1})

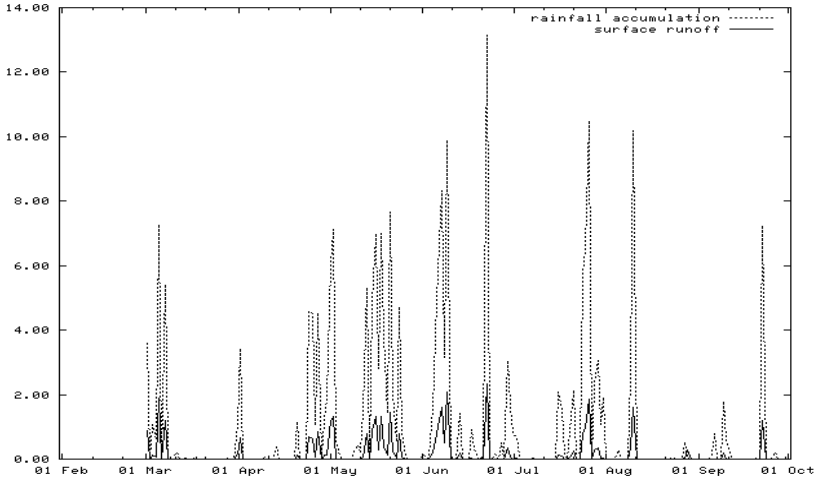

(c) Gridsquare Mean potential and actual Evaporation (mm day^{-1})

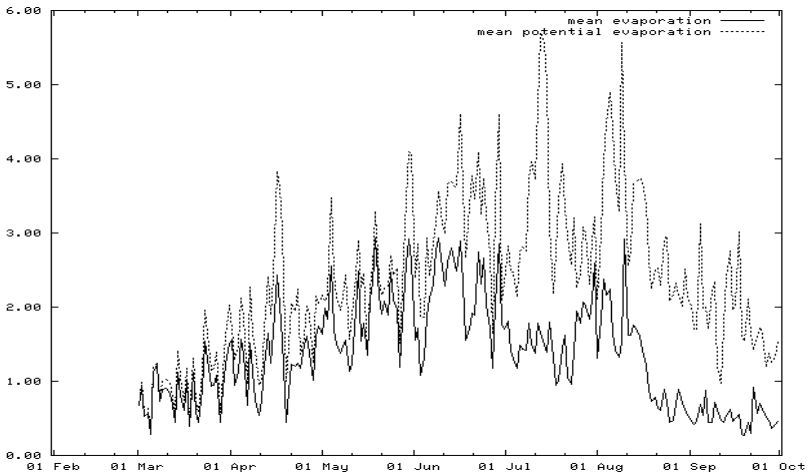

(d) Median soil moisture deficit (mm)

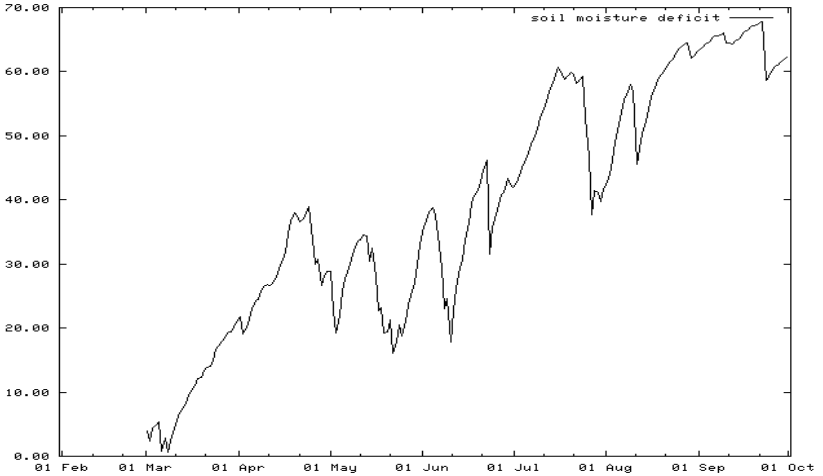

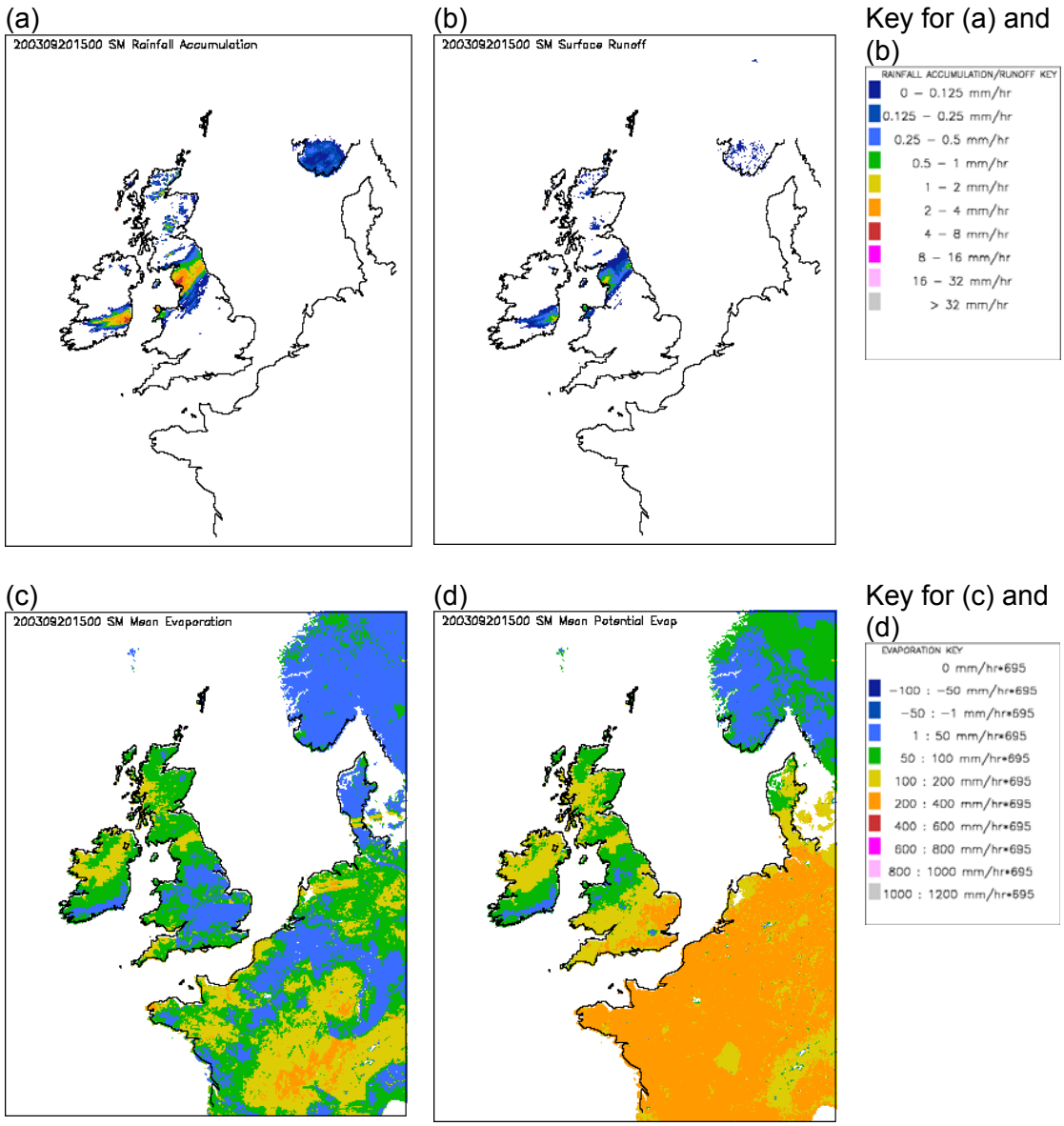

Figure 5. Maps of (a) accumulated rainfall (mm hr^{-1}), (b) surface runoff (mm hr^{-1}), (c) actual evaporation and (d) potential evaporation (mm hr^{-1} x 695 ≈ W m^{-2} latent heat) as calculated by Nimrod-MOSES-PDM for the hour 14:00-15:00 GMT on 20 September 2003.

(a)

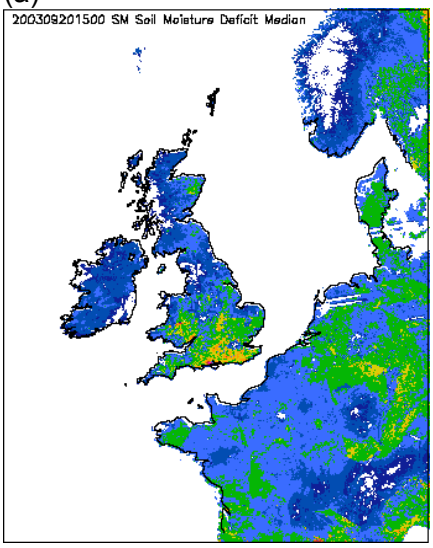

(b)

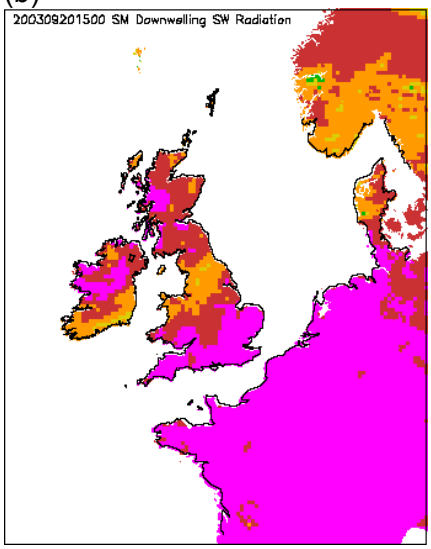

Key for (a)

Key for (b)

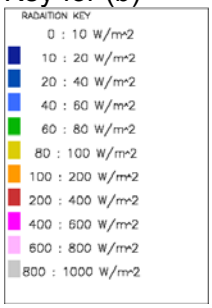

Figure 6. Maps of (a) soil moisture deficit for a median soil (mm) at 15:00 GMT and (b) mean downward solar radiation (W m^{-2}) for the hour 14:00-15:00 GMT on 20 September 2003 as calculated by Nimrod-MOSES-PDM.

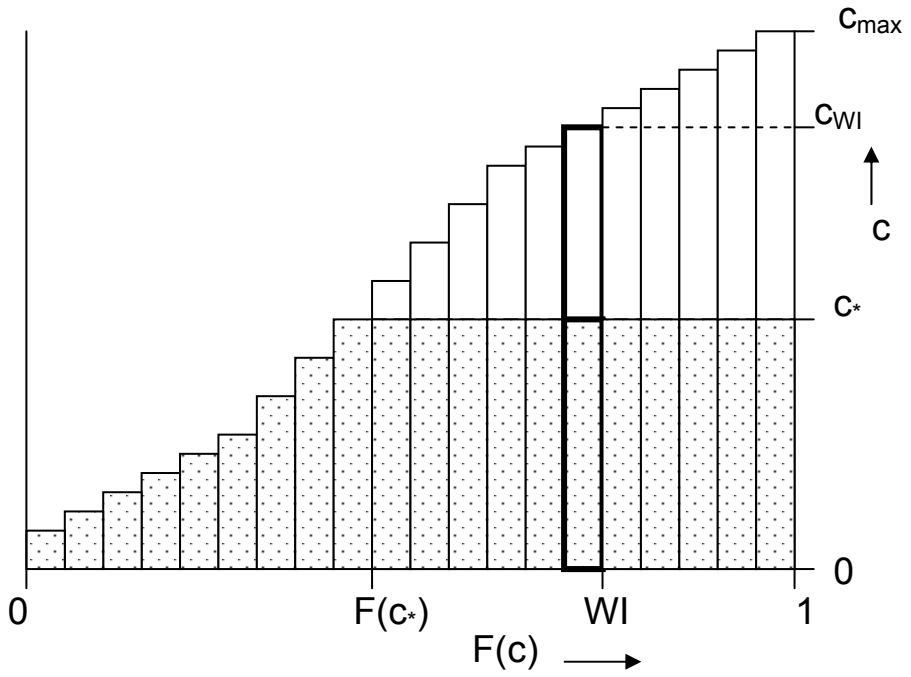

Figure 7. The PDM scheme (see Figure 2 and Section 2.3 for definitions of c, c_{max}, c_* and F(c)), showing the water holding capacity, c_{WI}, corresponding to the wetness index, WI (column shown in bold). The stippled area represents saturated soil. The fraction of the water holding capacity for the wetness index WI that is saturated determines the MOSES-PDM soil moisture concentration corresponding to WI as a fraction of its saturated value.

5. Summary and Future Developments

This paper has explained how the Met Office Surface Exchanges Scheme (MOSES) has been modified by including the Probability Distributed Moisture (PDM) scheme to take into account heterogeneity in soil properties when calculating surface runoff. It has also shown how MOSES-PDM has been implemented in the Met Office Nimrod nowcasting system to:

- Use Nimrod's analyses of precipitation, precipitation type, cloud amounts and near-surface atmospheric variables to produce hourly inputs to MOSES-PDM,
- Use high-resolution soil and land surface characteristics data as ancillary fields for MOSES-PDM,
- Produce hourly updated values of snowmelt, runoff, net surface radiation, evaporation, potential evaporation, soil temperature, soil moisture and soil moisture deficit on a 5km resolution grid.

Nimrod-MOSES-PDM runs every hour on the operational Nimrod hardware at the Met Office. A comparison of outputs from MOSES-PDM and MORECS as well as some further verification studies are underway.

Future work to enhance this soil state and surface hydrology system include:

- Use of near real-time remotely sensed vegetation cover and Leaf Area Index (LAI) in place of the currently specified seasonal variation of vegetation parameters,
- Replacement of the soil hydraulics component of MOSES-PDM with the van Genuchten formulation (van Genuchten, 1980) so that soils data specified in terms of the van Genuchten parameters can be used directly,
- Allowing for the heterogeneity of snow cover within a gridsquare due to unresolved surface elevation variations,
- Routing the runoff produced by MOSES-PDM to enable verification via river flow data where flow gauges are in place and to produce estimates of river flow and possible flooding area in ungauged catchments.

It may also be possible and desirable to assimilate net radiation data and estimates of soil moisture from remotely sensed microwave brightness temperatures into the model.

Acknowledgements

The authors would like to thank Brian Golding for producing the initial idea and plans for the work reported here and for his continuing support and encouragement, Martin Best and Richard Essery for providing much technical advice on MOSES, Chris Taylor for helping with the calculation of soil characteristics ancillary fields and Vicky Bell and Bob Moore for helpful discussions about PDM. The work was funded by the Meteorological Support Group of the UK Ministry of Defence under the Trafficability component of their Research and Technology Programme.

References

Allen, R.G., Smith, M., Pereira, L.S. and Perrier, A., 1994: An update for the

calculation of reference evapotranspiration. *ICID Bulletin*, **43**(2), 35-92.

Arnfield, A., 1979: Evaluation of empirical expressions for the estimation of hourly and daily totals of atmospheric long-wave emission under all sky conditions. *Quart. J. Roy. Meteorol. Soc.*, **105**, 1041-1052.

Bell, V.A. and Moore, R.J., 1998: A grid-based distributed flood forecasting model for use with weather radar data: Part 1. Formulation*. Hydrology and Earth Systems Science*, **2**(2-3), 265-281; Part 2. Case studies, **2**(3), 283-298.

Blyth, E.M., 2002: Modelling soil moisture for a grassland and woodland site in south-east England. *Hydrology and Earth Systems Science*, **6**(1), 39-47.

Brutsaert, W., 1975: Atmospheric emissivity. *Water Resources Research*, **11**, 742-744.

Burke, E.J. and Simmonds, L.P., 2001a: Passive microwave emission from smooth bare soils: developing a simple model to predict near surface water content. *International. J. of Remote Sensing*, **22**(18), 3747-3761.

Burke, E.J. and Simmonds, L.P., 2001b: A simple parameterisation for retrieving soil moisture from passive microwave data. *Hydrology and Earth Systems Science*, **5**(1), 39-48.

Carson, D.J., 1982: Current parameterisations of land-surface processes in atmospheric general circulation models*. Land Surface Processes in Atmospheric General Circulation Models*, Eagleson, P.S. (Ed.), Cambridge University Press, UK.

Clapp, R. and Hornburger, G., 1978, Empirical equations for some soil hydaulic properties. *Water Resources Res.*, **14**, 601-604.

Cox, P.M., Huntingford, C. and Harding, R.J., 1998: A canopy conductance and photosynthesis model for use in a GCM land surface scheme. *J. Hydrol*., **212**, 79-94.

Cox, P.M., Betts, R.A., Bunton, C.B., Essery, R.L.H., Rowntree, P.R. and Smith, J., 1999: The impact of new land surface physics on the GCM simulation of climate and climate sensitivity. *Climate Dynamics*, **15**, 183-203.

De Roo, A.P.J., Gouweleeuw, B., Thielen, J., Bartholmes, J., Bongioannini-Cerlini, P., Todini, E., Bates, P.D., Horritt, M., Hunter, N., Beven, K., Pappenberger, F., Heise, E., Rivin, G., Hils, M., Hollingsworth, A., Holst, B., Kwadijk, J., Reggiani, P., Van Dijk, M., Sattler, K., Sprokkereef, E., 2003: Development of a European flood forecasting system. *Intl. J. River Basin Management*, **1(**1), 49-59.

Dolman, A.J. and Gregory, D., 1992: The parametrization of rainfall interception in GCMs. *Quart. J. Roy. Meteorol. Soc.*, **118**, 455-469.

Essery, R.L.H., Best, M.J., Betts, R.A., Cox, P. M., and Taylor, C. M., 2003: Explicit representation of subgrid heterogeneity in a GCM land-surface scheme. *J. Hydrometeorology*, **4**, 530-543.

Fread, D.L., 1985: Channel Routing. In M.G. Andersen and T.P. Burt (eds.), Hydrological Forecasting. Chapter 14, J. Wiley, 437-503.

Fuller, R.M., Groom, G.B., Jones, A.R., 1994: The Land Cover Map Of Great Britain - An automated classification of LANDSAT Thematic Mapper data. *Photogramm. Eng. Rem.* **S 60**, 553-562

Global Soil Data Task Group, 2000: Global Soil Data Products CD-ROM (IGBP-DIS). [Global Soil Data Products CD-ROM (International Geosphere-Biosphere Programme - Data and Information System)]. CD-ROM available from Oak Ridge National Laboratory Distributed Active Archive Center, Oak Ridge, Tennessee, U.S.A. [http://www.daac.ornl.gov]

Golding, B.W.,1998: Nimrod: A system for generating automated very short range forecasts. *Meteorol. Appl*. **5**, 1-16

Goovaerts, P., 1997: Geostatistics for Natural Resource Evaluation. Oxford University Press, Oxford, UK.

Haurwitz, B., 1948: Insolation in relation to cloud types. *J. Meteorol.*, **5**, 110-113.

Hess, R., 2001: Assimilation of screen-level observations by variational soil moisture analysis. *Meteorol. Atmos. Phys*., **77**, 145-154.

Hough, M.N. and Jones, R.J.A., 1997: The United Kingdom Meteorological Office rainfall and evaporation calculation system: MORECS version 2.0 - an overview. *Hydrology and Earth System Sciences*, **1**(2), 227-239.

Hubrechts, L. and Feyen, J., 1996: Pedotransfer functions for thermal soil properties. Institute for Land and Water Management, Universiteit Leuven, pp.57.

Kasten, F., 1966: A new table and approximation formula for the relative optical air mass. *Arch. Meteorol. Geophys. Bioklimatol*., **B14**, 206-213.

Kitchen, M. and Harrison,D.L., 2001: Long-term trends in the accuracy of radar estimates of precipitation. Proceedings of the Fifth International Symposium on Hydrological Applications of Weather Radar, Kyoto, Japan, 245-250.

Lenhard, R.J., Parker, J.C. and Mishra, S., 1989: On the correspondence between Brooks-Corey and Van Genuchten models*. J. Irrigation and Drainage Engineering*, **115**, 744-751.

Loveland, T.R., Reed, B.C., Brown, J.F., Ohlen, D.O., Zhu, J, Yang, L., and Merchant, J.W., 2000: Development of a Global Land Cover Characteristics Database and IGBP DISCover from 1-km AVHRR Data*: Int. J. Remote Sensing,* **21**, 1303-1330.

Miller, J.R., Russell, G.L. and Caliri, G., 1994: Continental scale river flow in climate models*. J. Climate*, **7**, 914-928.

Moore, R.J., 1985: The probability distributed principle and runoff production at point and basin scales. *Hydrol. Sci. J.*, **30**(2), 263-297.

Oki, T., Agata, Y., Kanae, S., Saruhashi, T., Yang, D. and Musiake, K., 2001: Global assessment of current water resources using total runoff integrating pathways*. Hydrol.I Sci. J.*, **46**(6), 983-995.

Price, M., 1996: Introducing Groundwater, Second Edition, Chapman & Hall, London,

Rhodin, A., Kucharski, F., Callies, U., Eppel, D.P. and Wegen, W., 1999: Variational soil moisture analysis from screen-level atmospheric parameters: Application to a short-range weather forecast model. *Quart. J. Roy. Meteorol. Soc*., **125**, 2427-2448.

Richards, L., 1931, Capillary conduction of liquids through porous mediums. *Physics*, **1**, 318-333.

Sausen, R., Schubert, S. and Dumenil, L., 1994: A model of river-runoff for use in coupled atmosphere-ocean models*. J. Hydrology*, **155**, 337-352.

Seuffert, G., Wilker, H., Viterbo, P., Mahfouf, J.-F., Drusch, M. and Calvet, J.-C., 2003: Soil moisture analysis combining scree-level parameters and microwave brightness temperature: A test with field data. *Geophys. Res. Letters*, **30**(10), 1498-1502.

Thompson, N., Barrie, I.A. and Ayles, M., 1981: The Met Office Rainfall and Evaporation Calculation System MORECS*. Met Office Hydrological Memorandum No. 45.* Unpublished report available from the National Meteorological Library, London Road, Bracknell, RG12 2SZ, UK.

Thornley, J.H.M., and Johnson, I.R., 1990: Plant and Crop Modelling. Oxford University Press, UK, pp.669.

van Genuchten, M.T., 1980. A closed form equation for predicting the hydraulic conductivity of unsaturated soils. *Soil Society of America Journal*, **44**, 892-898.

Warrilow, D.A. and Buckley, E., 1989: The impact of land surface processes on the moisture budget of a climate model. *Annales Geophysicae*, **7**,439-450.

Wilson, M. F. and Henderson-Sellers, A., 1985: A global archive of land cover and soils data for use in general cieculation climate models. *J. Climatology*, **5**, 119-143.

Wright, B.J. and Thomas, N., 1998: An objective visibility analysis and very-short-range forecasting system. *Meteorol. Appl.*, **5**, 157-181.

Yu, Z., Lakhtakia, B., Yarnal, R.A., White, D.A., Miller, D.A., Frakes, B., Barron, E.J., Duffy,C. and Schwartz, F.W., 1999: Simulating the river-basin response to atmospheric forcing by linking a mesoscale meteorological model and hydrologic model system. *J. Hydrology*, **218**, 72-91.